ORIGINAL ARTICLE

Field investigation of force and displacement within a strata slope using a real-time remote monitoring system

Jiangbo Xu[1] · Heng Li[1,2] · Ke Du[1] · Changgen Yan[1] · Xu Zhao[1] · Wu Li[2] · Xinzhuang Xu[2]

Abstract

Research on monitoring and forecasting technology for slope stability is important for ensuring railway operation. This paper presents field investigation of force and displacement within a strata slope using a real-time remote monitoring system. Based on the interactions of the landslide body, the landslide bed and the monitoring anchor of slope, the mechanical principle of relative movement between the landslide body and the landslide bed can be found. This paper puts forward stress data obtained from a monitoring anchor as the main criterion for landslide stability. The stress will change continually inside the slope mass before the occurrence of a landslide. When the sliding force is larger than the anti-sliding force, deformation and landslides will occur; thus, the change in stress occurs before the change in displacement. In this study, the internal stress, deep displacement and surface strain of a railway slope were measured by a real-time remote-monitoring system, and a vibration metre was installed on the surface of the railway slope to study the influence of the train vibration load on the stability of the slope. The monitoring results are synthetically analysed temporally and spatially, then a railway slope forecasting model is proposed. According to the railway slope field application, the forecasting model makes successful predictions.

Keywords Real-time remote monitoring · Railway slope forecasting model · Slope internal stress · Train-induced vibration

Introduction

With the development of China's transportation infrastructure and the promotion of operational safety awareness, research on predicting the stability and deformation of railway slopes subjected to micro-quakes has aroused interest among scholars. Vibrations from passing trains will damage the rock mass, undoubtedly affecting the stability of nearby slopes. Thus, it is important to monitor the influences of the vibrations from passing trains, especially in soft rock slopes.

With the rapid development of transportation, more and more engineering projects are occurring on soft rock slopes. This trend has been recognized as a worldwide problem since the 1960s, and stability is one of the most common challenges for rock slope engineering. The main soft rock slope appearances include steep slopes, low slope height,

large slope length and structural plane development. Soft rock is a special type of rock, and because of its nature and vulnerability, its slope stability is difficult to control. Researchers are fully aware of the significant damage caused by the deformation instability of soft rock slopes in soft rock. Controlling the deformation of soft rock slopes in engineering has, therefore, become more and more important, and thus, more and more attention has been paid to the stability of rock slopes. Some researchers have carried out relevant research. For example, Pereira and Lana (2013) performed elastic and plastic simulations, studied the strength and deformability parameters of open-pit mines with buckling failure, and their influences on the buckling failure mechanism in global open-pit mine slopes was explored. This research provided an important contribution to establish the basic conditions for this kind of failure. Chen et al. (2015a, b) studied the influence of rock mass properties on slope stability based on slope failures during the Wenchuan earthquake that happened in 2008, and found that rock falls and debris flows are likely to occur in the harder rock masses, and that landslides are likely to occur in the areas covered by softer rocks. Lee and Bae (2015) investigated 79 sites where slope collapse occurred during or immediately after

✉ Jiangbo Xu
xujiangbo@yeah.net

[1] School of Highway, Chang'an University, Xi'an 710064, China

[2] Institute of Science and Technology, Xi'an Railway Bureau, Xi'an 710054, China

construction in the Chungcheong region, and evaluated their geometric characteristics, the collapse characteristics, and some design and reinforcement methods. The geologic, climatic and environmental characteristics were found to have affected the stability of slopes. It was found that the development of joint (55%) is a major factor of slope destruction. Zhu et al. (2013) investigated carbonaceous phyllite, the weak layer widely distributed in the Yunfu pyrite of Guangdong Province. The deformation characteristics and strength properties of the carbonaceous phyllite rock mass were analysed through laboratory uniaxial and triaxial compression tests. Silva and Lana (2012) evaluated the influence of durability on the phyllite physical properties through slake durability tests of phyllite with different alteration grades and strengths. With regard to open-pit slopes, instead of multi-factor monitoring of landslide geologic hazards, He (2009) made a single-sliding force mechanical quantity monitoring based on the principle of the interaction force of a sliding body, sliding bed and monitoring anchor cable and developed a remote monitoring and warning system that was applied on site. Chen et al. (2015a, b) analysed the degeneration characteristics of the rock slope from the water inlet slope of the Huangjinping Hydropower Station, and studied the causes of natural and engineering slope cracks. To study the stability and deformation of soft rock high slopes during excavation and rainfall, Xiao et al. (2007) conducted the physical simulation and analysed the relationship between slope deformation of the slope and the supporting structure. Based on the unloading rock mass mechanics theory, Deng et al. (2009) analysed the excavation unloading of high soft rock slopes using the geotechnical numerical analysis software ADINA. These authors compared the analysis results with the monitoring results under the same working condition, and verified the rationality of the calculation and analysis. Fu et al. (2012) studied the impact of rainfall infiltration upon slope stability and proposed a new calculation method considering both the effect of the seepage field and the soft rock. Chen et al. (2013) studied the pre-stress loss of anchor cables applied to ensure slope stability in soft rock slope engineering, and discovered the quantitative loss law of pre-stressed anchor cables that provides a reference to slope support engineering for to strengthening slope stability. The slope safety problem has become more and more serious, and some scholars have studied slope stability problems with monitoring. Qu et al. (2016) developed a robust methodological approach using the "hybrid-SAR technique" to promptly identify diverse landslides with different deformation magnitudes, sliding modes and slope geometries, and provided reliable data support for the forecasting and monitoring of landslides. Nolesini et al. (2016) used remote sensing techniques to research Volterra, a town of great historical interest in Central Italy. They analysed the displacements occurring both in the urban areas and the surrounding

slopes and detected possible critical sections with instability phenomena. Palenzuela et al. (2016) proved the usefulness of remote monitoring techniques achieved by light detection and ranging (LIDAR) in quantifying the ongoing change in the terrain, as well as in comparisons between digital terrain models. Zhang et al. (2009) analysed the monitoring results of high-slope excavation on the left bank of the Jinping Cascade-I Hydropower Station, and studied the impact of slope rock mass excavation and the stability of the slope after excavation unloading. Ma et al. (2014) analysed the monitoring results of slope displacement to determine the position and shape of the potential slip surface that provides the basis for slope stability analysis. To accurately forecast slope stability, Hu et al. (2016) adopted the support vector machine (SVM) to establish the nonlinear relationship between slope stability and its influencing factors. Li (2015) used the method of least squares support vector machines to train and simulate the slope displacement–time data. The quantum-behaved particle swarm optimization (QPSO) optimizes the parametres of the LSSVM model to avoid artificial arbitrariness and enhance the forecast accuracy. Based on the GIS platform combined with a multivariate non-equidistance grey forecast model, Xu et al. (2014) developed a set of early warning systems for open-pit slope disasters. Huang et al. (2017) selected the Qinglingou Slope located at the head of the Three Gorges Reservoir as a case study and a UAV (Unmanned aerial vehicle)-based remote sensing method was applied to monitor this steep mountainous slope. Carla et al. (2017) used ground-based radar to monitor and characterize typical slope deformation behaviour, and defined the appropriate strategy for offsetting up alarms. Uchimura et al. (2015) proposed a simple monitoring method for the early warning of rainfall-induced landslides and mainly monitored tilt angles in the surface layers of the slope.

Remote monitoring is an efficient and convenient detection method for monitoring slope status and for mastering slope engineering. Few studies on the relationship between train vibrations and slope disasters on railway slopes have been conducted, although some slope disasters have been caused by train vibrations. On November 24, 2014, a landslide accident occurred on the Xiangfan–Chongqing railway that caused the derailment of an eight-carriage train and killed two drivers (Figs. 1, 2). To study the relationship between train vibrations and slope slides, a potential landslide site was selected and remote monitoring was performed 2 km away from the accident site. The slope conditions are similar to the geological conditions at the accident site.

From the railway safety operation point of view, the role of slope engineering monitoring is more and more significant. Regardless of the factors that cause the slope failure, the final manifestation is the force and deformation, and thus, the study of slope deformation characteristics is important. In this paper, the deformation characteristics of

Fig. 1 Train derailment caused by a landslide () Cited from the network
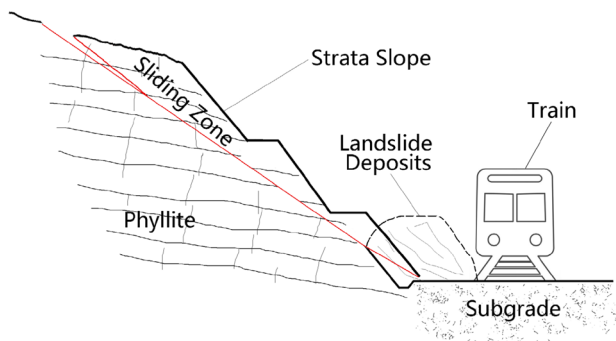

Fig. 2 Sliding mechanism diagram

a phyllite slope and its dynamic deformation characteristics caused by train vibrations were studied.

Methodology

As a natural mechanical system, the occurrence of a landslide depends on the equilibrium state between the slip and anti-slip forces. A landslide is the process from gradient increase to final failure. The forward shear force (the forward sliding force) before sliding can be used as a sufficient and necessary condition to predict the landslide. Thus, real-time monitoring of the forward sliding force can predict the occurrence of a landslide. The advantage of the monitoring system is to determine the essential characteristics of slope instability through real-time monitoring of the disturbing force and then to calculate the sliding force of the landslide (He 2009).

In fact, a landslide is a form of disaster movement in which the slip body moves along the sliding surface. When the sliding force is the main factor, sliding occurs. When the slip force is a secondary factor, the landslide is stable. The key to landslide monitoring prediction is to grasp the dynamic change of the sliding and anti-sliding forces. The landslide mechanical system as a "natural mechanical system" cannot directly monitor its advanced sliding force, so we must adopt technology that will transform a "natural mechanical system" into a "measurable mechanical system". A small disturbing force is applied through the anchor cable that passes through the sliding surface (Fig. 3). The disturbing force is called "percussion". Once the percussion force has been involved in the landslide mechanical system, relationship between it and the sliding force can be derived, reflecting the change of the forward sliding force.

Sliding friction:

$$F_{\varphi} = (P_n + G_n)\tan\overline{\varphi} + cl.$$

In the limit equilibrium state,

$$\sum \overline{X} = 0,$$

$$P_t + F_{\varphi} - G_t = 0,$$

$$G_t = P_t + F_{\varphi}.$$

The mathematical expression of the advanced sliding force G_t is

$$G_t = P\left[\cos(\alpha + \theta) + \sin(\alpha + \theta)\tan\overline{\varphi}\right] + G\cos\alpha\tan\overline{\varphi} + \overline{C}l.$$

where G_t is the forward sliding force (kN); P is the disturbing force (kN); G is gravity (kN); α is the angle between the sliding surface and the horizontal plane (°); θ is the angle of the monitoring anchor cable (°); ϕ is the weighted average of the internal friction angle of each soil layer in the sliding slope (°); C is the weighted average of the cohesion for each layer of the sliding surface (kN); l is the sliding surface length (m); and G_n is the normal force (kN). In addition, P is the measurable force of the man-made mechanical system, and the unpredictable sliding force G_t can be expressed as a function of P, which can be calculated.
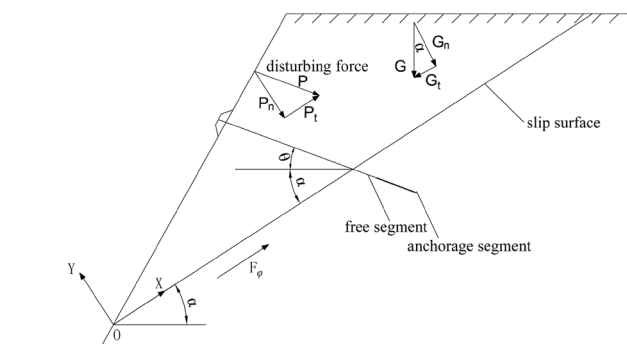

Fig. 3 Mechanical model of a landslide

The engineering situation

Location

The site is a slope disaster area located on the left side of sections K252 + 894 ~ +920 of a railway line, and there is a 200-m^3 collapsed body in front of the slope at sections K252 + 900 ~ +920. In November 2014, cracks continued to expand after a heavy rainfall, and the widest crack reached up to 0.5 m. Above the passive protection network at sections K252 + 920 ~ +975, the slope protection masonry suffered from bulging deformation. The slope seriously impacted the operational safety of this railway, so it is critical to monitor it to provide early risk warnings.

Geological survey

1. *Geological settings* The lithology of the area is strongly weathered quartz mica schist, and the deformation developed towards the railway line at an inclination of 40°–67°. The rock mass is cross-cut by structural planes and multiple sets of unfavourable joints and levels, all of which provided the structural conditions for the formation of sliding. Under the action of natural forces such as rainwater erosion and plant root splitting, it was likely that various unfavourable structural planes would develop further, which would lead to sudden geological disasters and threaten the safety of the railway operation.
2. *Topography and geomorphology* The disaster slope is located on the right bank of the Han River at sections K252 + 900 ~ 975. The terrain is higher on the left and lower on the right, and the natural cross-slope is steep (40°–50°).
3. *Formation lithology* Engineering geological surveys and drilling showed that the formation is composed of Quaternary Holocene silty clay and Silurian quartz mica schist (Fig. 4).
4. *Geological structure* The railway line runs from east to west, and the tendency of the rock strata is from east to west, and the rock formation developed towards the railway line. Due to the influence of the regional geological structure, the inclination angle of the rock stratum changed rapidly. The tectonic conditions for the sliding disaster might be caused by shattered slope rock masses or uneven rocks in structural planes.

Physical properties

The mechanical parameters of each layer under natural and saturated conditions are listed in Table 1.

Table 1 Mechanical parameters of each layer under natural and saturated conditions

Layer	Condition	γ/(kN m^{-3})	c/(kPa)	φ/(°)
Silty clay	Natural	18	10	28
	saturated	20	5	23
Weathered phyllite	Natural	20.5	30	31
	saturated	21.5	18	29
Strong weathered phyllite	Natural	23	43	33
	saturated	25	40	30

Fig. 4 Slope stratigraphic distribution
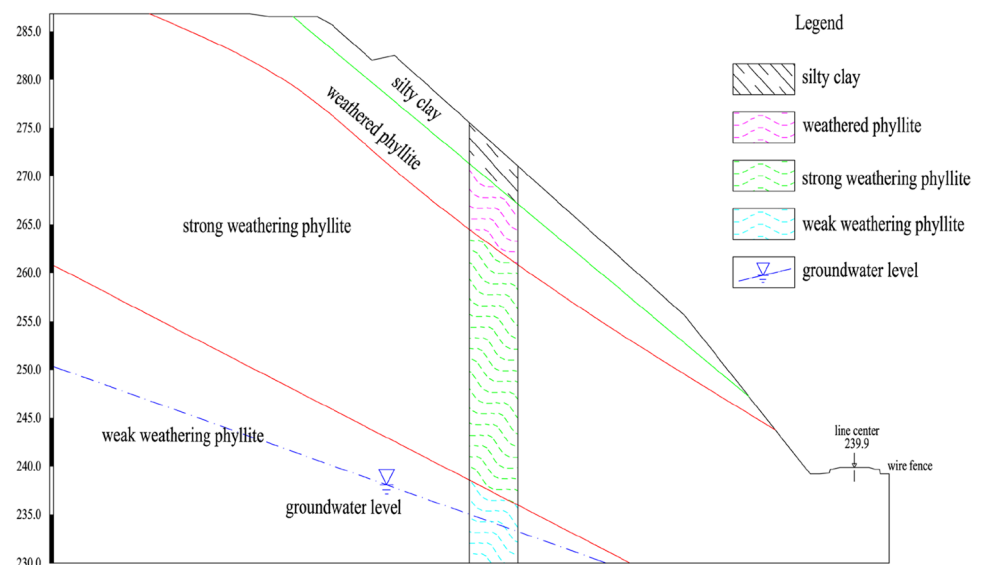
Remote monitoring

Monitoring content

The stress and deformation characteristics of the slope is studied to forecast sliding, specific monitoring results are shown in Table 2.

Instruments layout

Based on the design principle of a monitoring programme and considering the actual situation of the slope, the monitoring instruments were arranged along miles K252+915, K252+925 and K252+934. The slope monitoring instrument layout is shown in Fig. 5.

1. Monitoring instrument layout along mile K252+915

    The slope of mile K252+915 suffered a collapse. The slope cracks had a tendency to expand. Five steel metres

Table 2 Statistics of monitoring instruments

Monitoring items	Monitoring instrument	Main specifications	Remarks
Deep displacement	Multi-point displacement metre	Range: 1000 mm; resolution ≤ 0.03% F.S.; comprehensive error ≤ 2.0% F.S.	With mortar wrapped, fixed on the rock surface
Internal stress	Steel metre	Range: stress 100 MPa; tensile stress 200 MPa; precision: compression ≤ 0.12%F.S., subjected to tension ≤ 0.06% F.S.	Buried with 80 mm drilling holes which were 6 m deep
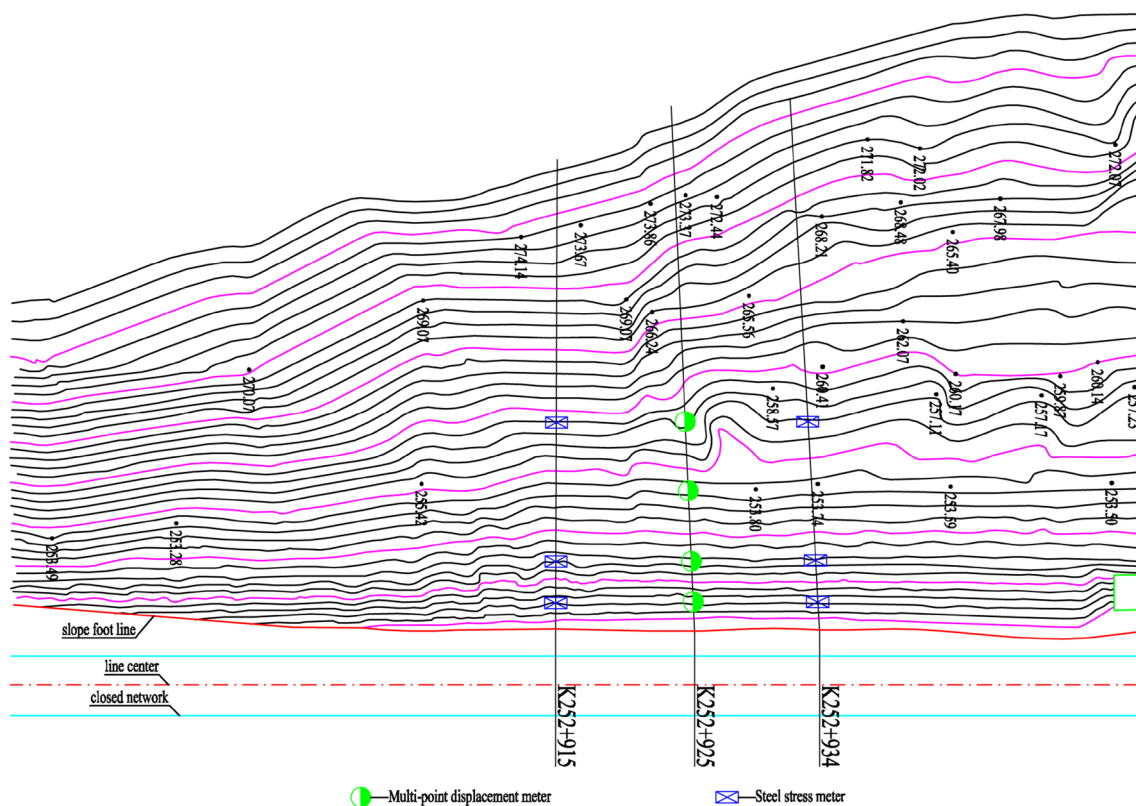
Fig. 5 Layout of the monitoring instruments

were arranged along the slope from the bottom to top. The instrument layout is shown in Fig. 6. Table 3 shows the monitoring instrument layout.

2. Monitoring instruments layout along mile K252 + 925

The location of this mile is the main landslide area of the slope. Four sets of three-point displacement metre were arranged along the slope from bottom to top. The layout of the instruments is shown in Fig. 7. Table 4 shows the monitoring instrument layout.

3. Monitoring instrument layout along mile K252 + 934

Five steel metres were arranged along this mile from bottom to top. The layout of the instruments is shown in Fig. 8. Table 5 shows the layout of the monitoring instruments.

4. Remote monitoring system

The remote monitoring system consists of the solar power supply system, the monitoring components, the signal transmission line, the signal automatic acquisition instrument, the signal remote wireless transmission equipment, the data centre (server) and the computer equipment for remote control instrument and data reading and analysis. The monitoring instruments adopted in the study are the vibrating string type, a 32-channel signal acquisition instrument is used for data remote transmission through the wireless network, making it possible to transfer and save monitoring data in real time as well as to read and process data through the terminal server device (Fig. 9).

Table 3 Monitoring instrument layout along mile K252 + 915

Monitoring instrument	Monitoring point no.	Monitoring point height (m)	Instrument buried depth (m)
Steel metre	D1	2	1
	D2	5	2
			4
	D3	15	2
			4

Results and analysis

Data processing and analysis of the steel metres

Choquet et al. (2017) describes some experiences about long-term stability and reliability of different kinds of vibrating wire instruments such as pressure sensor, strain gage and displacement transducer. The string-type steel metres are adopted to acquire the data in the form of a frequency value, and the frequency is converted into force value by the following formula:

$$P = k\left(f_i^2 - f_0^2\right),$$

where P is the force (kN) of the steel metre; k is the sensitivity coefficient (kN/Hz^2); f_0 is the initial frequency (Hz); and f_i is the working frequency (Hz).

The monitoring results from the steel metres arranged along mile K252 + 915 (D2) is analysed. The distribution of internal stress at different depths of the slope is shown in Fig. 10. It was found that the internal stress of the slope increased constantly during the first 2 months of the monitoring period. Thereafter, the internal stress becomes stable.
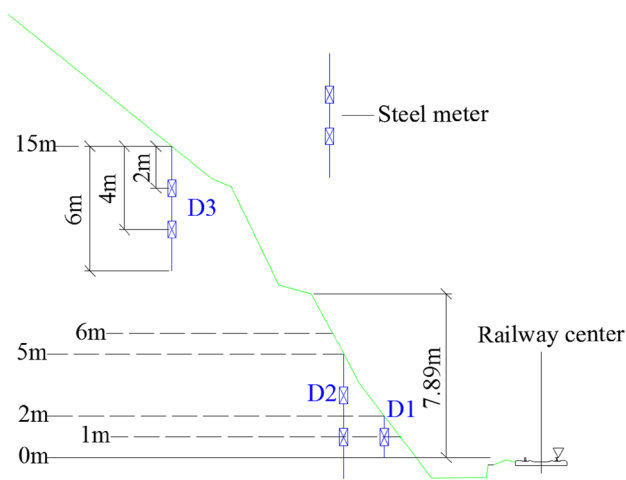

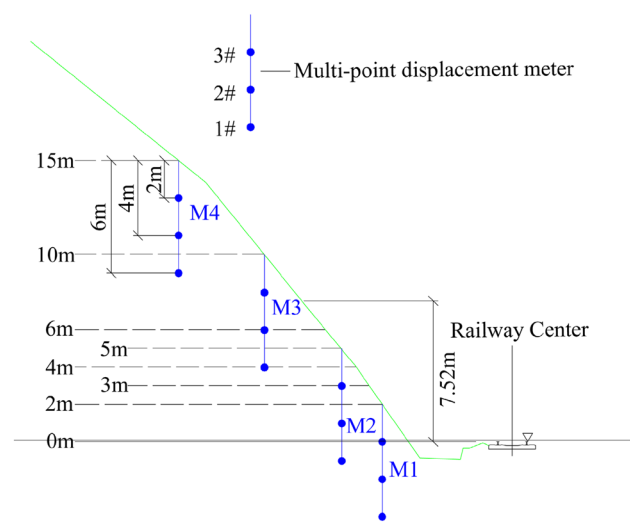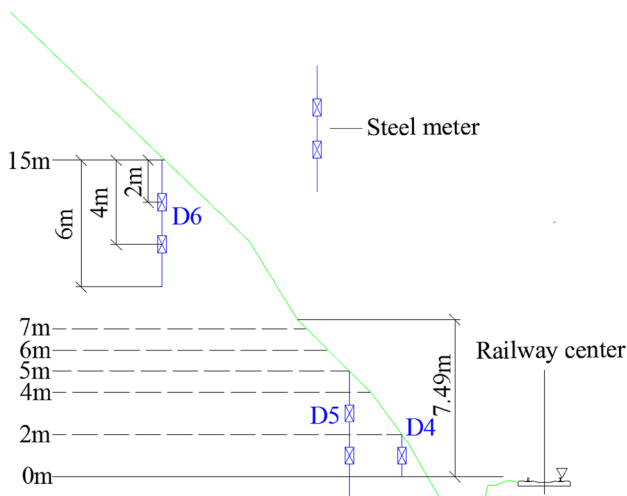**Fig. 6** Monitoring instrument layout along mile K252 + 915

Fig. 7 Monitoring instrument layout along mile K252 + 925

Table 4 Monitoring instrument layout along mile K252+925

Monitoring instrument	Monitoring point no.	Monitoring point height (m)	Instrument buried depth (m)
Three-point displacement metre	M1	2	1#–6
			2#–4
			3#–2
	M2	5	1#–6
			2#–4
			3#–2
	M3	10	1#–6
			2#–4
			3#–2
	M4	15	1#–6
			2#–4
			3#–2

Fig. 8 Monitoring instrument layout along mile K252+934

Table 5 Monitoring instruments layout along mile K252+934

Monitoring instrument	Monitoring point no.	Monitoring site height (m)	Instrument buried depth (m)
Steel metre	D4	2	1
	D5	5	2
			4
	D6	15	2
			4

Then, the force changes little and the internal stress of the slope tends to be stable, and the force values monitored at the depth of 2 m were obviously greater than the values at the depth of 4 m, but their variation curves were similar. Meanwhile, internal forces at depth of 2 m with different height (D1, D2 and D3) are monitored along mile K252+915 which are shown in Fig. 11. It is clear that, the force of D1 of higher location is larger than that of D3 with lower location, and the internal slope stress is getting smaller from bottom to top.

Data processing and analysis of multi-point displacement metre

Multi-point displacement metres are arranged on the main sliding mile K252+925. The internal slope displacement at different depth of monitoring point M2 is analysed as shown in Fig. 12. It shows that the displacement variation trend at different embedding depths is basically constant, and the displacement does not change greatly. The displacement at the depth of 6 m is the largest, approximately 0.08 mm. The displacement at the depth of 4 m is the smallest, close to 0 mm, and the displacement at the depth of 2 m is approximately 0.015 mm, whereas the monitoring results of other multi-point displacement monitoring points also showed a similar relative relationship. The displacement at 4 m is almost 0 mm, and there are small displacements at 6 and 2 m, this indicates that there are two potential sliding belts in this landslide. The first sliding belt is between 4 and 6 m. The second slide belts are located between 2 and 4 m. Combined with geological data, it is known that between 2 and 4 m is the interface of rock and soil.

Meanwhile, the monitoring result of multi-point displacement at point M1, M2, M3 and M4 are presented in Fig. 13 (taking the depth of 6 m as an example). It is clear from Figs. 12 and 13 that, very small variations of slope internal displacement can be found at stable condition, which is quite different from the result observed from the steel metres.

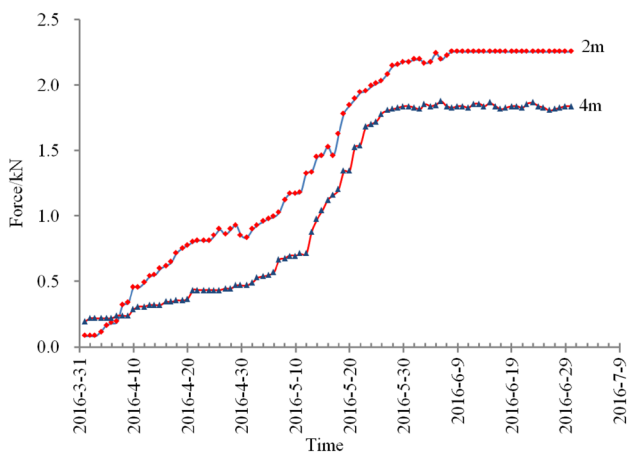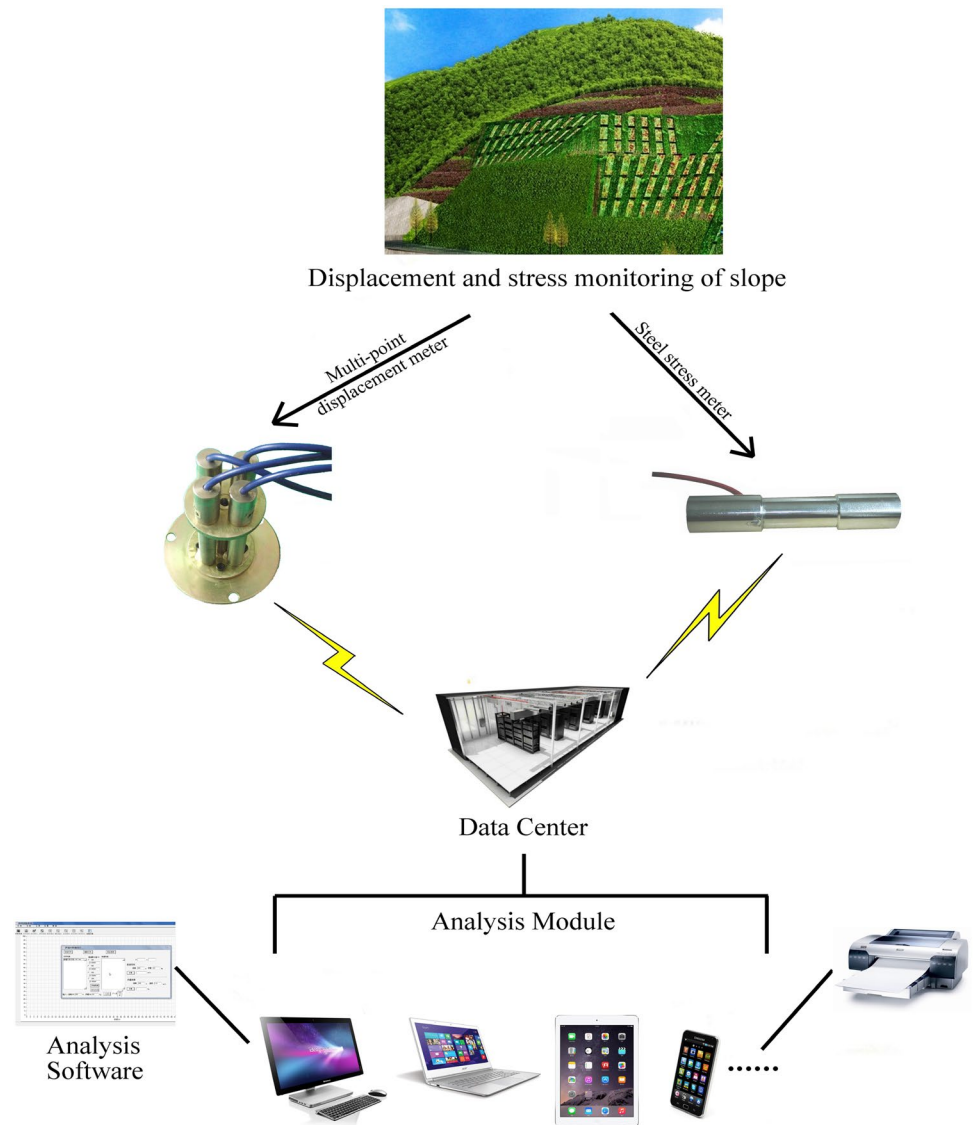**Fig. 9** Composition of the slope
monitoring system

Displacement and stress monitoring of slope

Multi-point displacement meter

Steel stress meter

Data Center

Analysis Module

Analysis
Software

· · · · · ·

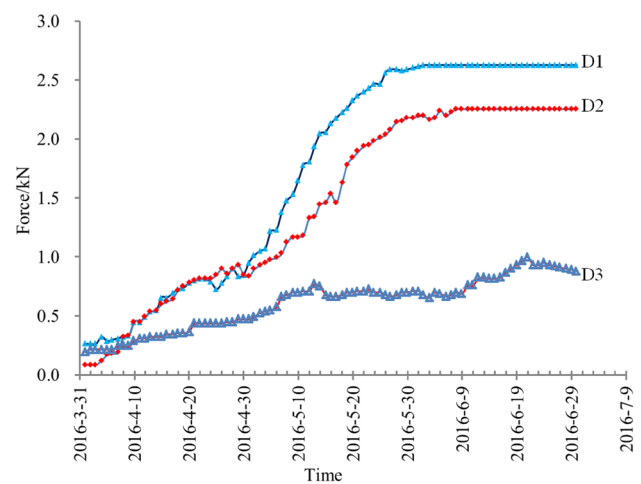**Fig. 10** Force–time curves of the steel metres at D2
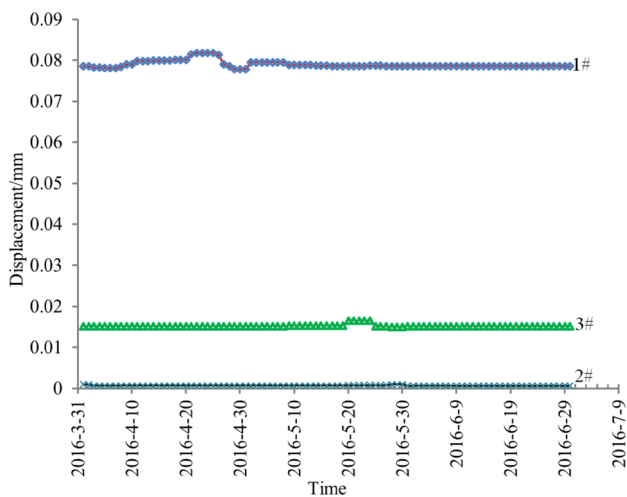

Fig. 11 Force–time curves of steel metres at D1, D2 and D3

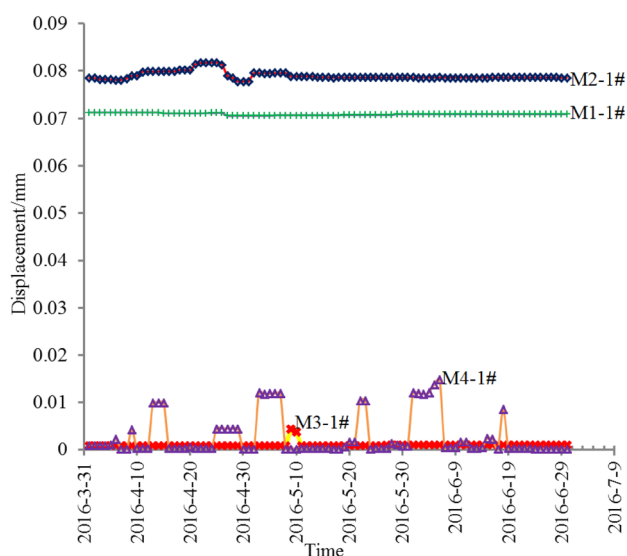**Fig. 12** Displacement–time curves of multi-point displacement metres at the measuring point M2

Fig. 13 Displacement–time curves of 1# displacement metres at the measuring points M1, M2, M3 and M4

The mechanism behind this is analysed based on the local geological condition. The slope surface is infiltrated by rainfall, which lead to the softening and breakage of surface rock, and a slight displacement is monitored at the depth of 2 m. After comparison and analysis of the monitoring results at depths of 4 and 6 m, it was found that the potential slip surface of the slope was between 4 and 6 m, leading to a more obvious displacement at 6 m and basically no change at 4 m.
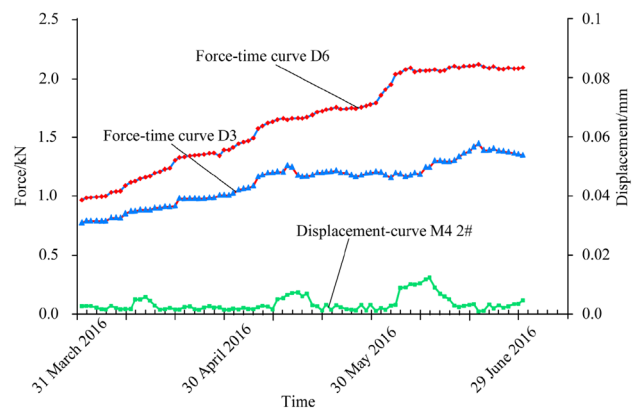
Fig. 14 The force–time and displacement–time curves of D3, D6 and M4 with depth of 4 m
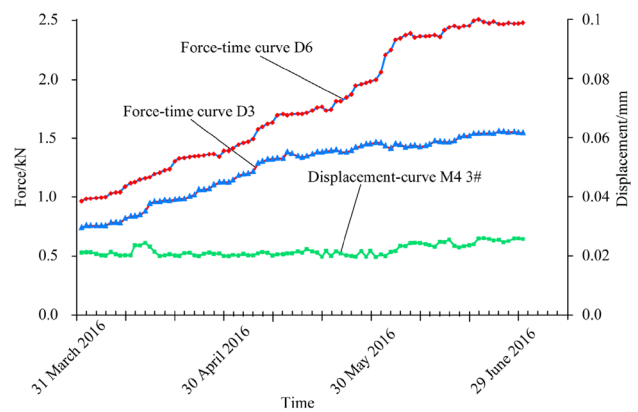

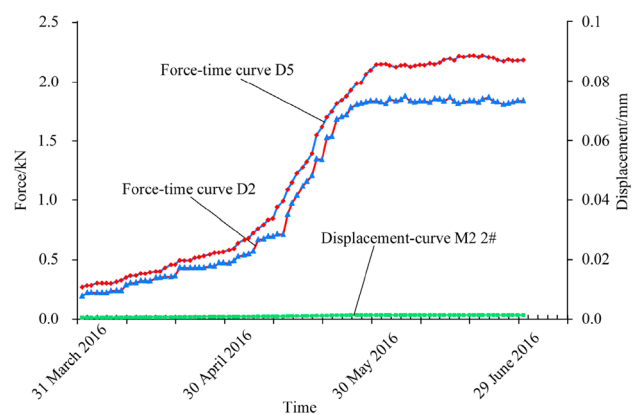**Fig. 15** The force–time and displacement–time curves of D3, D6 and M4 with depth of 2 m

Fig. 16 The force–time and displacement–time curves of D2, D5 and M2 with depth of 4 m

Comparison of displacement-based monitor and internal force-based monitor

The change of internal force and displacement at different depth and different points is compared which is shown from Figs. 14, 15, 16, 17 and 18. It is obvious that the change of stress happened much earlier than that of displacement. In terms of slope failure prediction, the monitoring of stress could be much reliable compared with the monitoring of displacement.

To validate the conclusion obtained, the monitoring data of slight landslide that happened on 24 September 2017 is captured as shown in Fig. 19.

In Fig. 19, the force time curve is the D2 data with a depth of 4 m, the displacement time curve is the M2 data with a depth of 4 m.

It is found from Fig. 19b that the change of internal force happened 2 days earlier than the displacement which is consistent with the result observed of stable slope. Meanwhile, the data mutation of internal force was observed on 21 September 2017, whereas the data mutation cannot be found in the displacement data, which shows the advantage of internal force-based monitoring system over the displacement-dependent system. In the force time curve, there is a steep rise in force, which is used to define the pre-warning criteria. Therefore, the pre-warning of landslide based on the internal force could effectively prevent the disaster from happening.

Conclusion

The monitoring system is adopted to precast the slope failure along the railway line from Xiangyu to Chongqing and the following conclusions have been drawn:
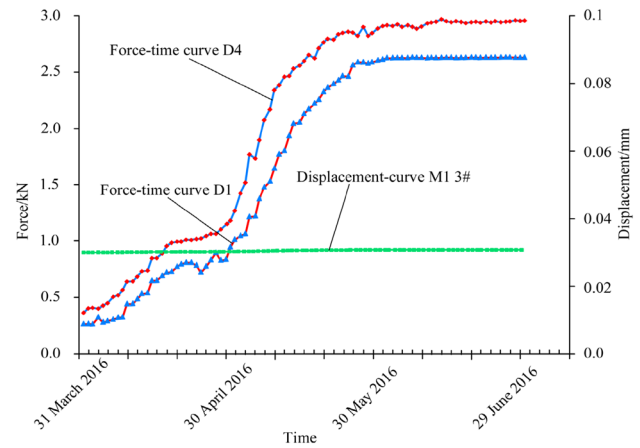
Fig. 18 The force–time and displacement–time curves of D1, D4 and M1 with depth of 1 m

1. When the sliding force is larger than the anti-sliding force of the rock mass, deformation and sliding may occur in the slope. The monitoring data show that the sliding force changes ahead of the displacement. The sliding force in the slope is more important for the slope early warning than the slope displacement.

2. Landslide mechanical model was established based on the "natural mechanical system" and the functional

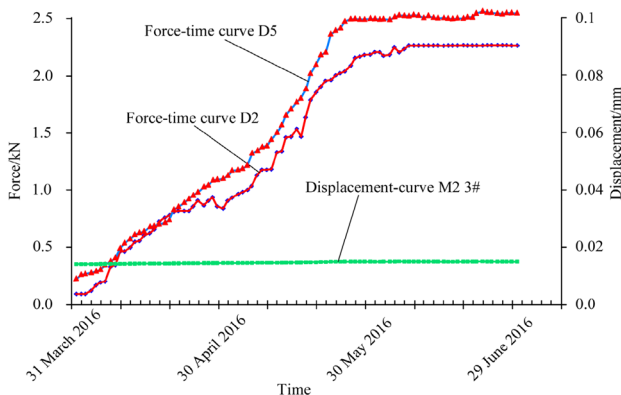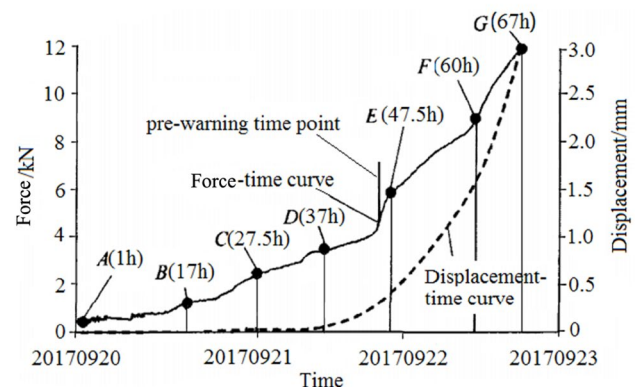**(a)** The slight landslide that occurred on September 24

Fig. 17 The force–time and displacement–time curves of D2, D5 and M2 with depth of 2 m

(b) The force-time and displacement-time curves before the slight landslide occurred

Fig. 19 Data gathered from the landslide

relation between the percussion and sliding forces was derived. The change of the forward sliding force is of great significance for accurate prediction of the landslide hazard.

3. Based on the result from internal force and displacement of slope, it is concluded that the internal force-based monitoring system can provide more timely and accurate response of slope stability compared with the displacement-based monitoring, which is also validated from the slight landslide.

Compliance with ethical standards

Conflict of interest The authors declare that there are no conflicts of interest regarding the publication of this paper.

References

Carla T, Farina P, Intrieri E, Botsialas K, Casagli N (2017) On the monitoring and early-warning of brittle slope failures in hard rock masses: examples from an open-pit mine. Eng Geol 228:71–81

Chen Y, Yin J, Hu Y (2013) Research on prestress quantitative loss law of soft rock slope anchor cable. Chin J Rock Mech Eng 32(8):1685–1691

Chen XL, Zhou BG, Ran HL et al (2015a) Influence of rock masses properties on the slope stabilities: a study based on slope failures during the 2008 Wenchuan earthquake. In: 12th International IAEG Congress, Torino, Italy, Engineering Geology for Society and Territory, vol 2: landslide processes, pp 1219–1223

Chen T, Deng J, Li L et al (2015b) Deformation characteristics and stability evaluation of a heavily loosened rock slope. Chin J Rock Mech Eng 34(S1):2607–2616

Choquet P, Juneau F, Debreuille PJ, Bessette J (2017) Reliability, long-term stability and gage performance of vibrating wire sensors with reference to case histories. In: Proceedings of the 5th International Symposium on Field Measurements in Geo-mechanics, Singapore

He M (2009) Real-time remote monitoring and forecasting system for geological disasters of landslides and its engineering application. Chin J Rock Mech Eng 28(6):1081–1090

Fu H, Zeng L, Wang G et al (2012) Stability analysis of soft rock slope under rainfall infiltration. Rock Soil Mech 33(8):2359–2365

Hu J, Wang K-K, Dong J-H (2016) Forecasting of slope stability based on BCABC-SVM. J Shenyang Univ Technol 38(2):222–227

Deng H, Li J, Yi Q et al (2009) Research on unloading deformation of soft rock high slope. Rock Soil Mech 30(6):1731–1734

Huang HF, Long JJ, Lin HY, Zhang L, Yi W, Lei BJ (2017) Unmanned aerial vehicle based remote sensing method for monitoring a steep mountainous slope in the Three Gorges Reservoir, China. Earth Sci Inform 10(3):287–301

Lee J, Bae W (2015) A case study on collapse characteristics of slope during construction in the Chung-Cheong area. J Korean Geoenvironmental Soc 16(10):23–32

Li Y (2015) Forecasting of slope displacement based on QPSO-LSSVM method. Mt Res 33(3):374–378

Ma M, Wang J, Li W et al (2014) Identification of potential landslide slippery surface morphology based on displacement monitoring data. Chin J Undergr Space Eng 10(6):1455–1461

Nolesini T, William F, Bianchini S et al (2016) Detecting slope and urban potential unstable areas by means of multi-platform remote sensing techniques: the Volterra (Italy) case study. Remote Sens 8(9):746

Palenzuela JA, Jimenez-Peralvarez JD, El Hamdouni R et al (2016) Integration of LiDAR data for the assessment of activity in diachronic landslides: a case study in the Betic Cordillera (Spain). Landslides 13(4):629–642

Pereira LC, Lana MS (2013) Stress-strain analysis of buckling failure in phyllite slopes. Geotech Geol Eng 31(1):297–314

Qu TT, Lu P, Liu C et al (2016) Hybrid-SAR technique: joint analysis using phase-based and amplitude-based methods for the xishancun giant landslide monitoring. Remote Sens 8(10):874

Silva CHC, Lana MS (2012) Influence of slake durability on geotechnical behavior of phyllites of Pau Branco Mine. Rem Rev Esc Minas 65(3):413–418

Uchimura T, Towhata I, Wang L, Nishie S, Yamaguchi H, Seko I, Qiao J (2015) Precaution and early warning of surface failure of slopes using tilt sensors. Soils Found 55(5):1086–1099

Xiao K, Zhou DP, Li H (2007) Physical modeling of deformation properties for soft rock slope under excavation. Rock Soil Mech 28(1):111–115, 122

Xu M, Guo Z, Li H (2014) Application of multivariable non-equidistance gray forecast model in open-pit slope disaster warning. Sci Survey Map 39(9):83–86

Zhang J, Weiya XU, Haiyuan JIN et al (2009) Safety monitoring and stability analysis of large-scale and complicated high rock slope. Chin J Rock Mech Eng 28(9):1819–1827

Zhu XX, Chen CX, Zheng Y et al (2013) Study of deformation and strength properties of the carbonaceous phyllite under natural and saturated condition. In: 3rd International-Society-for-Rock-Mechanics (ISRM) SINOROCK Symposium, Tongji Univ, Shanghai, Peoples R CHINA, pp 255–259